Dharali debris flow on 5 August 2025, Uttarakhand: event reconstruction and geomorphic implications

Vipin Kumar[1,*], Neha Chauhan[1], Abhisek Kumar Srivastav[1], Yaspal Sundriyal[1], Rajiv Sinha[2], Ravi Negi[3], Vikram Gupta[4], Akshaya Verma[5], Mohit Puniya[6] and Rahul Devrani[7]

[1]Department of Geology, Nityanand Himalayan Research and Study Center, Doon University, Dehradun 248 001, India
[2]Department of Earth Sciences, IIT Kanpur, Kanpur 208 016, India
[3]Geological Survey of India, Dehradun 248 001, India
[4]Department of Geology, Sikkim University, Gangtok 737 102, India
[5]National Institute of Hydrology, Roorkee 247 667, India
[6]Uttarakhand State Disaster Management Authority, Dehradun 248 001, India
[7]Jindal School of Environment and Sustainability, O. P. Jindal Global University, Sonipat 131 001, India

The Dharali debris flow on 5 August 2025, in Uttarakhand, India, was a catastrophic disaster that occurred in Kheer Gad, a tributary of the Bhagirathi river. It claimed approximately 60 lives and covered an estimated 3 hectares of apple orchards under debris. The damage also included at least 25–30 animals and a market comprising 65 hotels, over 30 resorts, and homestays. The present study involved the geomorphic characterisation of Kheer Gad to assess the debris flow potential of the catchment and debris flow simulation to ascertain the source, potential flow dynamics, and reconstruction. Findings reveal that the 17 km^2 Kheer Gad catchment is inherently unstable, as suggested by Melton's ruggedness number of 0.8, significantly above the 0.6 debris-flow threshold. The trigger was not a single event, but an antecedent rainfall of ~195 mm/30 days, which saturated glacial and landslide-derived source materials. Debris flow simulation revealed 60 kPa flow pressure, velocities of 5–10 m/s, flow height of 5–10 m, spread area of ~18 hectare, and volume estimate of 995,580 ± 200,000 m^3–1,285,260 ± 126,000 m^3. These values are validated against field observations. Notably, the disaster was exacerbated by human vulnerability, given the doubling of built-up structures between 2011 and 2025, despite prior warnings in 2013. The present study provides a transferable methodology for assessing similar high-risk, glaciated basins to prevent such avoidable disasters.

Keywords: Debris flow, Dharali, disaster risk reduction, Himalaya, rainfall.

HIMALAYA has been sensitive to global climate shifts, leading to glacial retreat and an increase in the frequency and intensity of extreme hydrometeorological events[1–4]. The North-Western Himalayas, particularly Uttarakhand, is one such region that has witnessed several disastrous hydrometeorological events, such as the 1970 Uttarakhand flood, 2013 Uttarakhand flood and landslides, and 2021 ice-rock avalanche and flood[5–8]. This pattern was further highlighted by the debris flow in Dharali on 5 August 2025, in the Kheer Gad catchment, a tributary of the Bhagirathi river in Uttarakhand, Himalayas. The event caused at least 60 deaths or missing persons, with the total toll reaching approximately 90 (ref. 9). This event led to the complete disruption of the National Highway (NH) 34, closing access to the Gangotri pilgrimage site and affecting rescue operations. Further, a subsequent debris flow event also occurred on the same day at Harshil village, which is 5 km downstream from Dharali, partially damming the Bhagirathi river and washing away part of an Indian defence camp. The frequency and scale of these hydrometeorological events support the notion of increasing vulnerability of the Indian Himalaya to a changing climate[10–13].

These events also mark a growing pattern of human-environment conflict, because population growth, increasing demand for agricultural land, growing tourist influx, and infrastructure expansion have led to encroachment on alluvial fans and river terraces in the Himalaya[14–17]. With numerous human settlements and infrastructure located in high-hazard zones in the Himalaya, predicting such debris flows is critical for disaster risk reduction. However, developing effective risk-reduction measures for such events requires a detailed understanding of the morphometry and hydrometeorological responses of the catchments. Drainage density, relief ratio, elongation ratio, and ruggedness number are among the basic morphometric parameters used to understand the debris-flow potential of catchments[18–22]. Further, various methods have been used to understand the hydrometeorological response of catchments, particularly regarding debris flow. These are empirical techniques[21], analytical methods[23], and advanced numerical models[24,25]. Among all these, numerical models have relative advantages owing to their flexibility in simulating events over complex terrains and in back-calculating key input parameters[26–28]. Given the

*For correspondence. (e-mail: v.chauhan777@gmail.com)

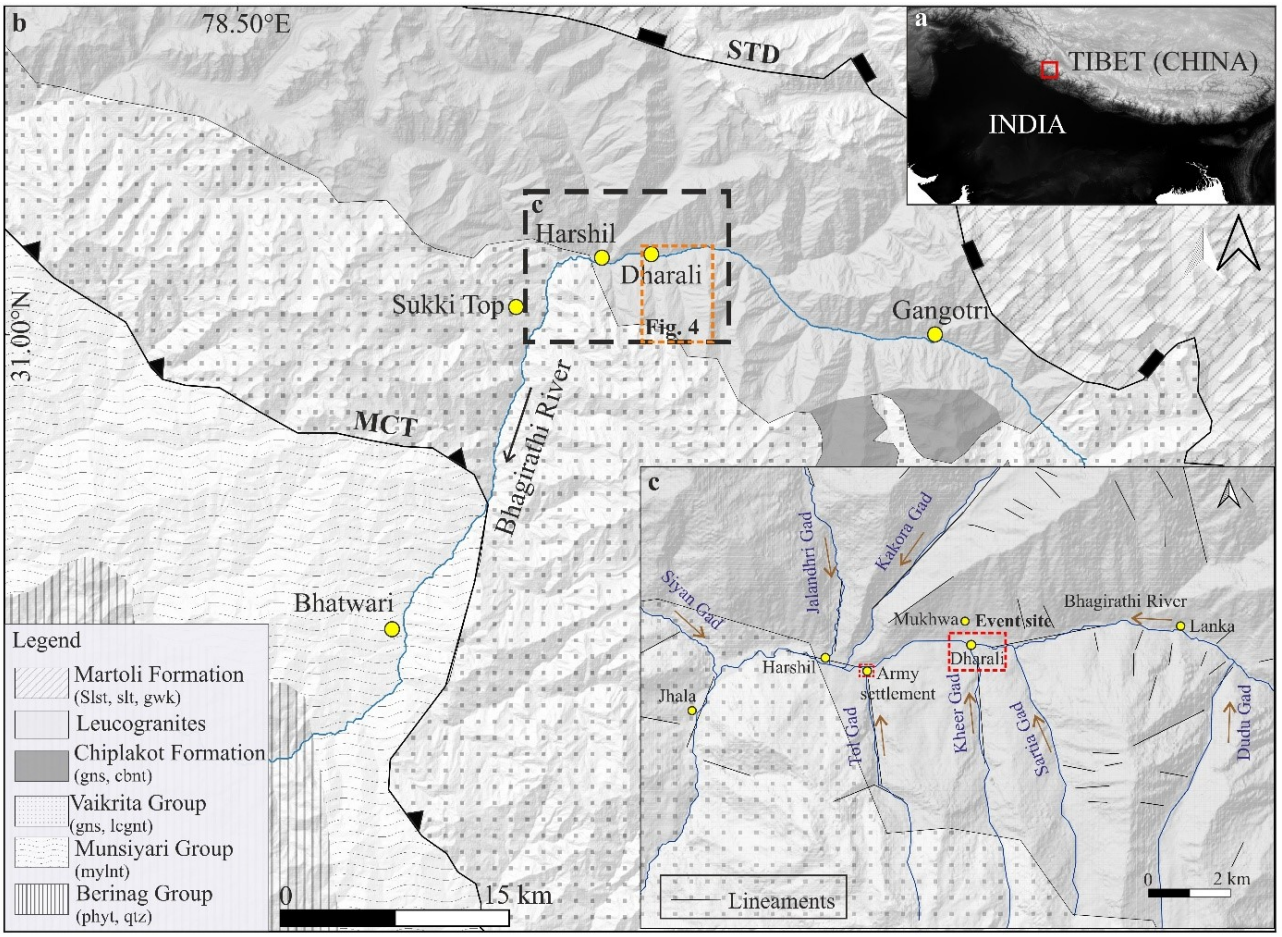

Figure 1. (*a*) Inset highlights the location of the study area, (*b*) Regional geology[29,30] (*c*) Tributary streams, lineaments. Yellow circles show the important locations. MCT, Main central thrust; STD, South Tibetan detachment; Slst, Silstone; Slt, Slate; Gwk, Greywacke; Gns, Gneiss; Cbnt, Carbonate; Lcgnt, Leucogranite; Mylnt, Mylonite; Phyt, Phyllite; Qtz, Quartzite.

devastating impacts of the 5 August 2025 Dharali debris flow, the present study aims at a post-disaster evaluation structured around two objectives: (i) geomorphic characterisation of Kheer Gad to assess debris flow potential of the catchment and (ii) debris flow simulation to ascertain the source, potential debris flow dynamics, and validation.

Study area

Dharali village, located at 31.0407° N latitude, 78.7972° E longitude at an elevation of 2,680–2,745 m along the left bank of the Bhagirathi river, is situated ∼20 km downstream from the Gangotri pilgrimage site in Uttarakhand, Himalaya, along NH 34 (Figure 1). This village is located at the mouth of Kheer Gad (a tributary of the Bhagirathi river). The hillslopes of this region comprise higher Himalayan crystalline rockmass[29,30]. The area has also suffered economic losses during the 2013 Uttarakhand flood[31].

Field observation

Figure 2 *a* and *b* represent the debris flow fan deposit made on the 5 August 2025 event and pre-disaster Google Earth (GE) imagery of the relict fan deposit, respectively. Pre-disaster imagery shows human settlements and apple orchards that were destroyed and buried under the debris from the 5 August 2025 event. Field observations in August 2025 and November 2025 revealed that during the 5 August event, debris flow was flowing ∼6 m above the present water level in the Kheer Gad channel before striking Dharali village (Figure 3 *a*). The flow deposits on the right, central, and left front represented a height of ∼3 m, 2 m, and negligible (merging at the Bhagirathi river), respectively (Figure 3 *b–d*). The dominant soil type of this debris flow deposit is sandy-silt (Figure 3 *e–f*). The opposite bank of the Bhagirathi river also got subjected to massive bank erosion caused by the event (Figure 3 *g*).

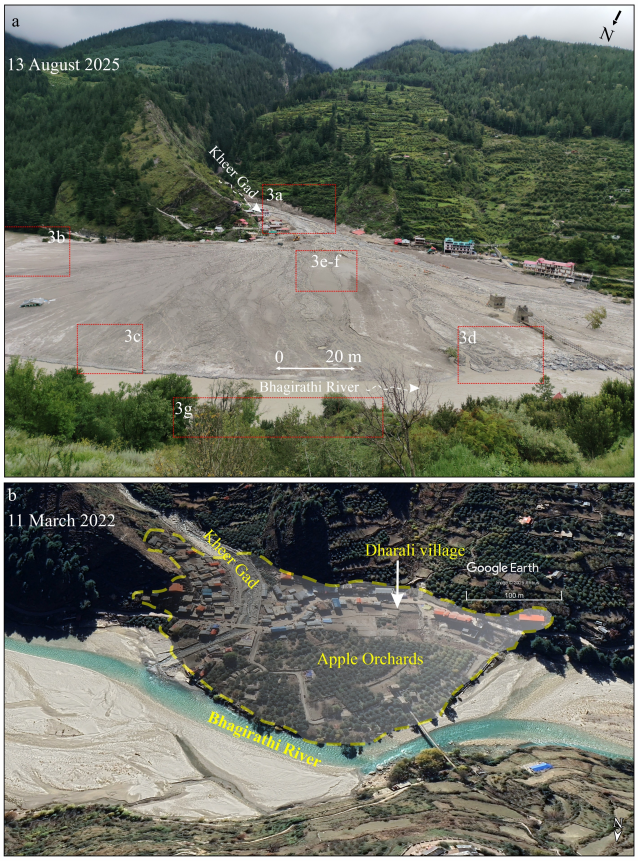

Figure 2. (***a***) Front view of the 5 August 2025 debris flow event, taken on 13 August 2025. Figure 3 (***a***–***g***) are depicted. Source: VK, RN, NC, and AS, (***b***) Pre-disaster imagery of 11 March 2022. Source: Google Earth (GE).

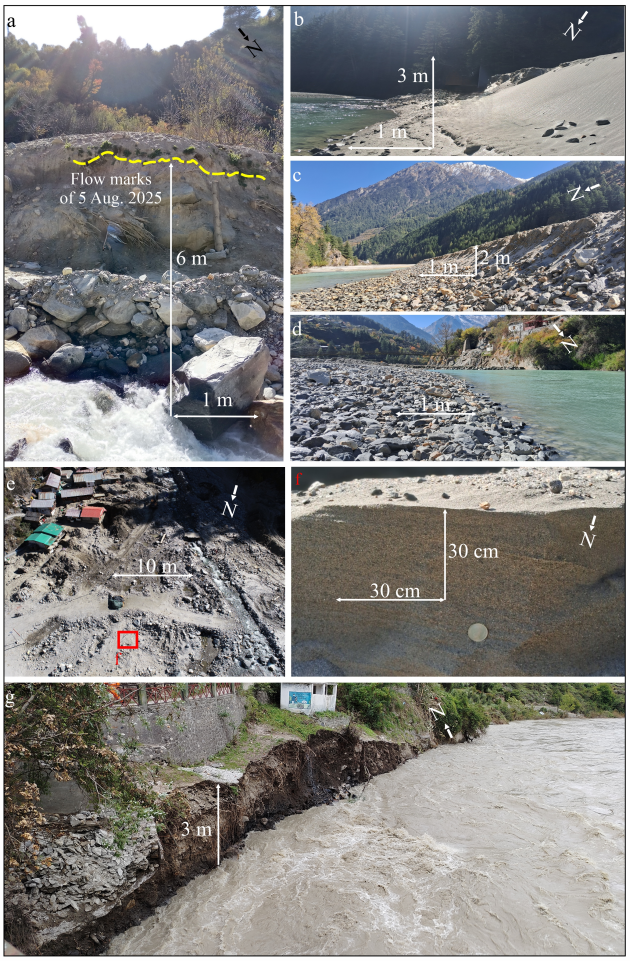

Figure 3. (***a***) Debris flow marks of the event at Kheer Gad mouth at Dharali village. (***b***) Right flank of the debris flow deposit. (***c***) Frontal part of the deposit. (***d***) Left flank of the deposit. (***e***) The central part of the deposit comprises the maximum thickness. (***f***) Sandy-silt soil accumulation highlights the flow's composition. (***g***) Right bank of the Bhagirathi river, opposite to the debris flow deposit, showing bank erosion.

Table 1. Input parameters for debris flow simulation

Input parameters	Depth (m)		Density* (kg/m^3)	Turbulence coefficient* (m/s^2)	Friction coefficient#	Total release area (m^2)	Total volume (m^3)
	Primary release (m)	Secondary release (m)					
Scenario 1	1	0.5	2000	600	0.08	617656	369464
Scenario 2	1.5		2000	600	0.08	1000156	1622611
Scenario 3	1	1.5	2000	600	0.08	1617812	1992075

* The estimation of density and flow turbulence was based on field observation of soil type (Figure 3 *f*) and also proposed by the following studies[17,26,33]. #Friction coefficient is the average slope of the deposition zone, which was determined from the topography.

Table 2. Catchment parameters, their source, and values obtained

Parameters	Source	Value
Area (A)	Digital elevation model (DEM)	17 km^2
Perimeter	DEM	22.55 km
Strahler stream order	DEM	4
Basin length (BL)	DEM	10.5 km
Total stream length (L)	DEM	46 km
Channel gradient	Elevation difference/Total length	260 m/km
Drainage density	L/A (m^{-1})	2.68 m^{-1}
Elongation ratio	(2/BL) *(A/π)	1.5
Relief ratio	(Basin elevation difference/ BL)	0.33
Melton's ruggedness number (MRn)	(Basin elevation difference/A)	0.8

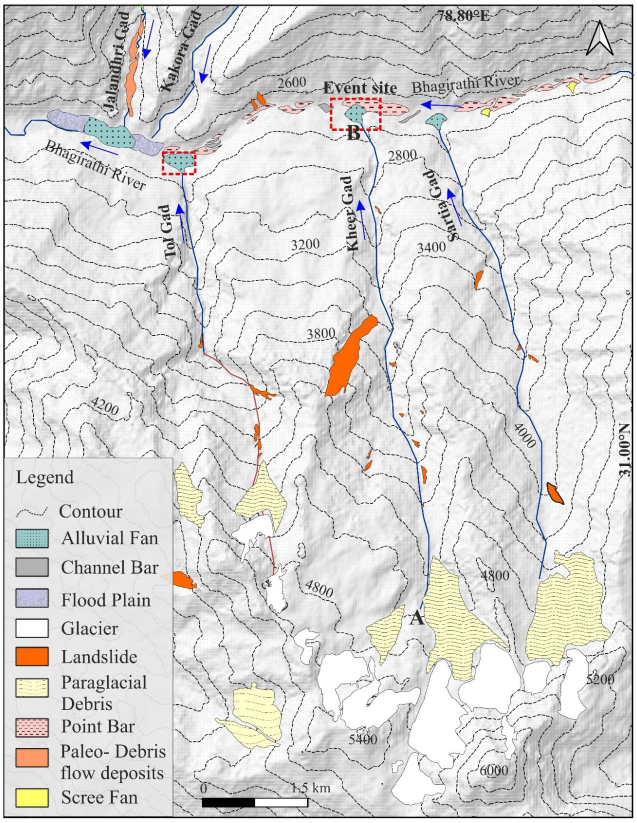

Figure 4. Spatial distribution of geomorphological features in the study area. The A–B section along the Kheer Gad channel is further explored in Figure 9. Mapping source: GE imagery of 11 March 2022.

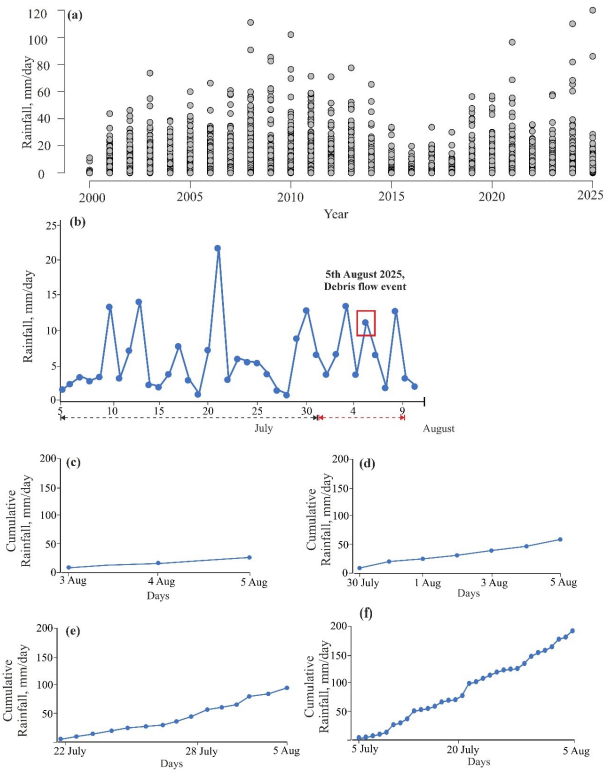

Figure 5. Rainfall pattern. (***a***) 2000–2025, daily rainfall data, (***b***) 5 July to 10 August 2025 daily rainfall data, highlighted rainfall on 5 August, (***c***–***f***) antecedent (3, 7, 15, and 30 days) rainfall plots.

Methodology

Geomorphological mapping and morphometric analysis

Geomorphological mapping was performed using high-resolution GE imagery of 11 March 2022 to identify and delineate key surface features, particularly the potential sediment sources within the Kheer Gad catchment. To quantify the inherent susceptibility of the catchment to rapid hydrological responses, such as debris flows, a morphometric evaluation was conducted. The key indices for this evaluation were as follows: drainage density, relief ratio, elongation ratio, and Melton's ruggedness number (MRn)[18–22].

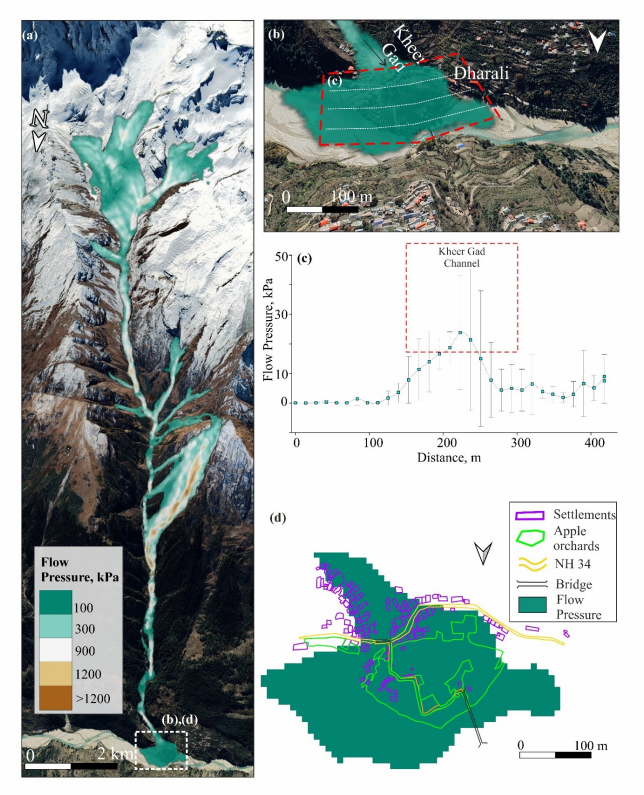

Figure 6. Debris flow pressure. (***a***–***b***) Flow pressure distribution. (***c***) Flow pressure variation across the spread over Dharali village. Error bars refer to the standard error of the mean in flow pressure corresponding to 3 sections (3 white lines inside red-dashed polygon (***b***)). (***d***) Spatial overlapping of flow pressure and land use features (mapped from 11 March 2022 GE imagery).

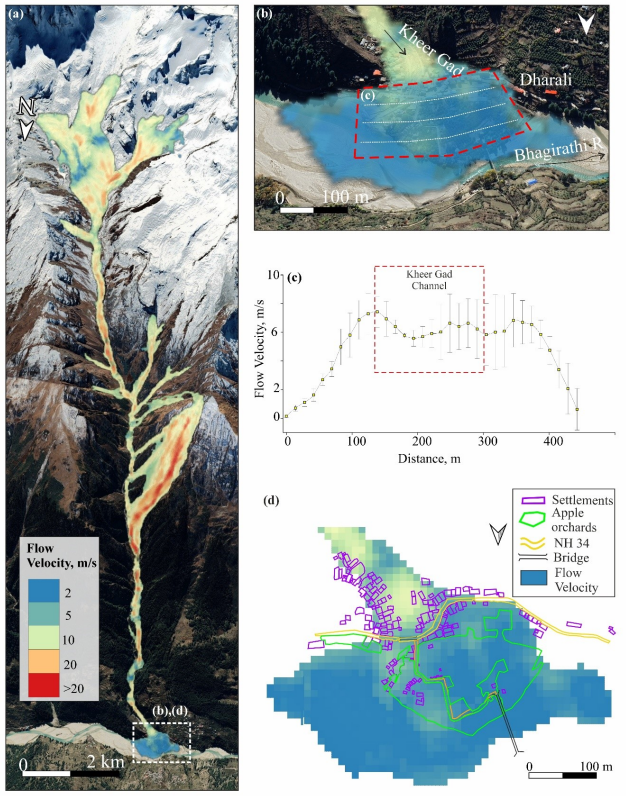

Figure 7. Debris Flow Velocity. (***a***–***b***) Flow velocity distribution. (***c***) Flow velocity variation across the spread over Dharali village. Error bars refer to the standard error of the mean in flow velocity corresponding to 3 sections (3 white lines inside red-dashed polygon in (***b***)). (***d***) Spatial overlapping of flow velocity and land use features (mapped from 11 March 2022 GE imagery).

Rainfall analysis

To investigate the event's triggering mechanism, we evaluated precipitation patterns using daily rainfall data (0.01° spatial resolution) from the FLDAS-Global model[32]. First, we analysed long-term rainfall patterns over the last 25 years (2000–2025) to provide historical context. Second, we analysed daily rainfall from 5 July to 5 August 2025 and calculated cumulative antecedent rainfall. This was done to assess its role in saturating the paraglacial and landslide material identified in the upper catchment.

Debris flow simulation

Debris flow simulation was performed to reconstruct the 5 August 2025 Dharali event, ascertain the potential source and depositional characteristics, and quantify flow velocity, pressure, flow height, and deposition. We used the Rapid Mass Movement Simulation (RAMMS) model, which is based on the Voellmy-Salm friction law[26]. RAMMS was chosen for its flexibility to incorporate key rheological criteria, multiple release areas, temporal settings, and flexible entrainment rates[14,17,33,34]. Utilising the findings from geomorphological mapping, multiple release areas, paraglacial deposits, landslides, and channel bank erosion were tested under the following three scenarios: Scenario 1- landslide only, Scenario 2- paraglacial only, Scenario 3- composite source (Table 1). This comparative approach allowed us to assess how different initiation zones influenced the final simulated event and determine which scenario best reproduced the observed characteristics of the event. These landslides and paraglacial features are shown on the geomorphological map (Figure 4).

Land-use mapping

To assess land-use damage, a temporal land-use map of Dharali village was prepared using satellite imagery (GE and Sentinel-2A) from 2011, 2014, 2016, 2018, 2020, 2022, and the latest, i.e., 2025 (ref. 35).

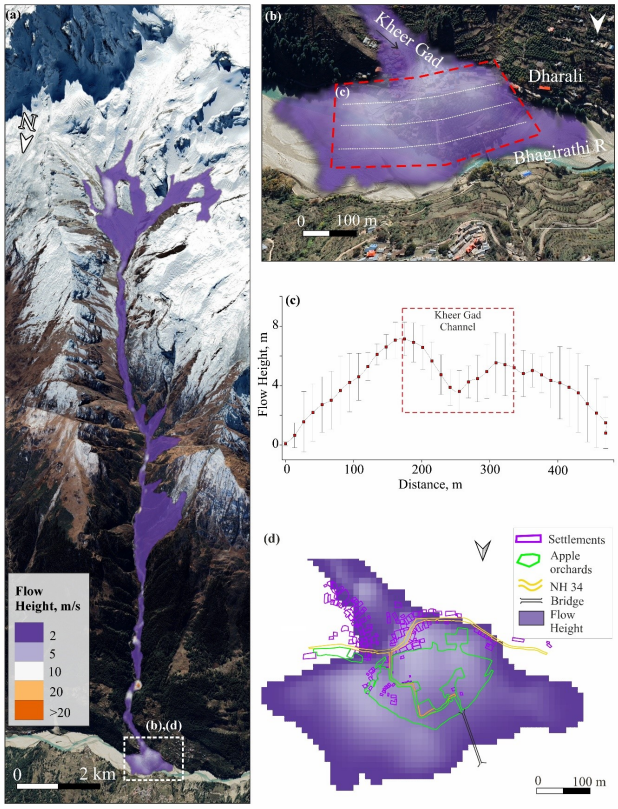

Figure 8. Debris flow height. (***a***–***b***) Flow height distribution. (*c*) Flow height variation across the spread over Dharali village. Error bars refer to the standard error of the mean in flow height corresponding to 3 sections (3 white lines inside red-dashed polygon (***b***)). (***d***) Spatial overlapping of flow height and land use features (mapped from 11 March 2022 GE imagery).

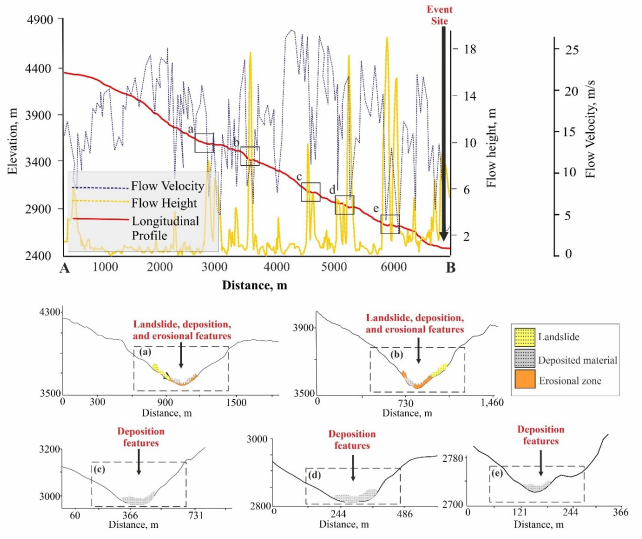

Figure 9. Flow height and velocity characteristics and channel morphology along the Kheer Gad channel (A–B). A–B section is shown in Figure 4. (***a***–***e***) Cross-section profiles corresponding to the five sites (Supplementary Figure 7), demonstrating varying channel width and evidence of active bank erosion, deposition, and lateral mass movement.

Results

Geomorphology and morphometric characteristics

The geomorphic mapping enabled the identification of features such as glacier extent, landslides (active and paleo), paraglacial debris, flood plain, alluvial fans, channel bar, and point bars (Figure 4). The values of morphometric parameters (Table 2) indicate that the 17 km^2 Kheer Gad catchment is inherently prone to debris flow generation. Another crucial factor is the abundant supply of both sediment and water from the catchment's glaciated area, which accounts for nearly 18% (~3 km^2) of the total basin. A critical finding confirming this is the MRn of 0.8, a value significantly above the 0.6 threshold widely recognised for debris flow-prone catchments[36,37]. The basins exceeding the MRn threshold, e.g., the study area, are frequently associated with impulsive, high-energy flows as opposed to moderate, flood-dominated systems[38]. This high-energy potential is reinforced by a steep channel gradient of ~260 m/km and a high relief ratio of 0.33. These metrics indicate the presence of steep, unstable slopes that are capable of rapidly mobilising sediment-laden flows during periods of intense runoff. Furthermore, the drainage density of 2.68 /m suggests a moderately dissected landscape, where water is quickly routed to the channel network, reducing infiltration and increasing the likelihood of rapid overland flow.

Rainfall regime

Analysis of daily precipitation data of 2000–2025 reveals an average of ~32.5 ± 2.5 mm/day for the site, and it is characterised by frequent rainfall events having values > 100 mm/day with some days recording up to 115 mm/day (Figure 5 *a*). Data reveals no extreme rainfall event on 5 August 2025 (Figure 5 *b*). However, antecedent rainfall over the last 3 days, 7 days, 15 days, and 1 month revealed that the area received 29 mm, 59 mm, 94 mm, and 195 mm, respectively (Figure 5 *c*–*f*).

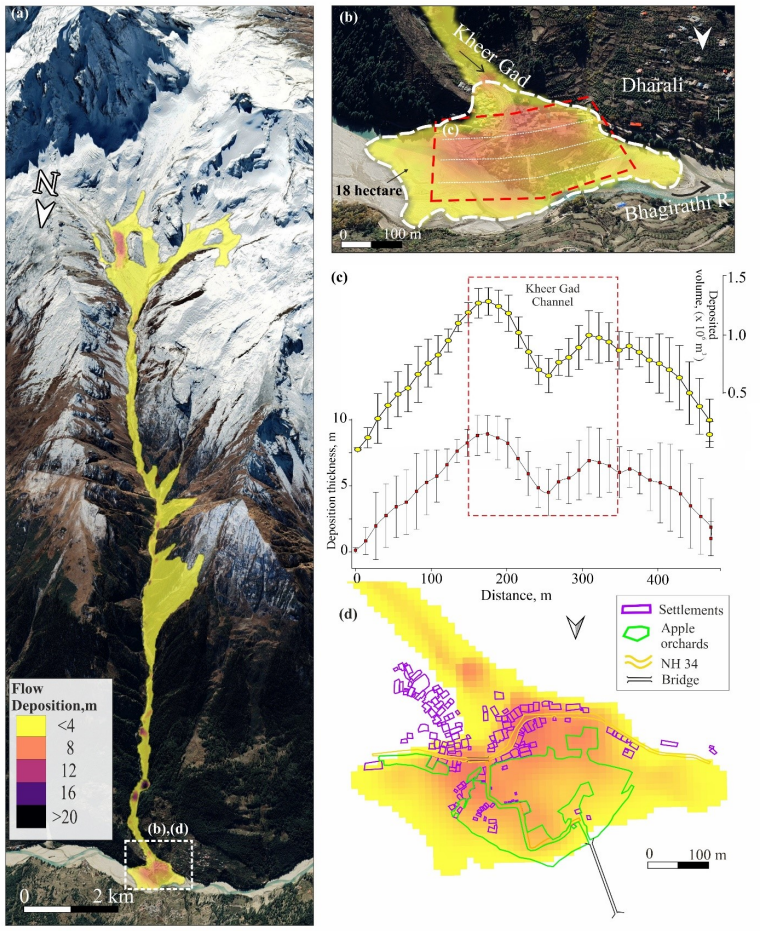

Figure 10. Debris Flow Deposition. (***a***–***b***) Deposition distribution. (***b***) Depositional area: 18-hectare (mapped by measuring the deposition spread from raster file in QGIS under WGS 1984-UTM 44 N zone projection). (***c***) Deposition thickness and deposited volume variation across the spread. Error bars refer to the standard error of the mean in deposition corresponding to 3 sections (3 white lines inside red-dashed polygon (***b***)). (***d***) Deposition underlain by various land-use elements.

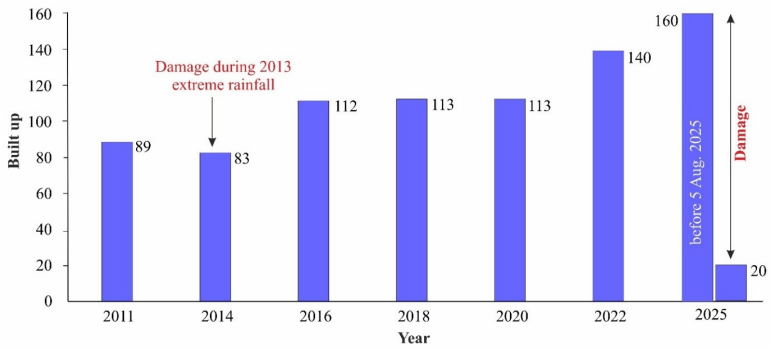

Figure 11. Built-up pattern at Dharali village during 2011–2025.

Debris flow simulation scenario

Three different simulation scenarios revealed that scenario 1 (landslide-only) and scenario 2 (paraglacial-only) are inconsistent with field reality (Supplementary Figures 1–6). However, scenario 3, which utilised a combined source (landslides and paraglacial debris), closely approximated the debris-flow characteristics of the 5 August 2025 event

(Figures 6–8). Further, the model was calibrated by varying the values of input parameters in scenario 3 (Supplementary Table 1) until the simulated debris flow extent and other debris flow characteristics matched the field reality. The model reveals the flow initiating at pressures of ~1200–1300 kPa, velocities up to 20≥ m/s, and flow height of 2–5 m in the upper part of Kheer Gad (Figures 6 *a*, 7 *a* and 8 *a*). At the mouth of the Kheer Gad where it struck Dharali, the flow retained pressures around ~60 kPa, velocities 5–10 m/s, and a flow height of 5–10 m (Figures 6 *b*, 7 *b* and 8 *b*). Cross sections across the flow pressure, velocity, and height spread, overlying the human settlement, NH 34, and orchard, reveal the values of 20.0 ± 10 kPa, 6.0 ± 1.5 m/s, 7.0 ± 1.5 m, respectively in the central part of deposit and diminish towards flanks (Figures 6 *c–d*, 7 *c–d*, 8 *c–d*).

Further, the flow pattern along the Kheer Gad channel reveals higher flow height values at certain sections (Figure 9 *a–e*). Frequent increased flow characteristics in the narrow sections, i.e., (Supplementary Figure 7) *a–b*, generally promote lateral erosion leading to landslides and channel erosion. It is further evident from the dominance of landsliding and channel erosion at (Supplementary Figure 7) *a–b*, as mapped using satellite imagery. However, at wider channel sections at the lower part of the Kheer Gad channel (Figure 10) *c–e*, higher flow characteristics contribute to sediment settling and deposition. This is also confirmed by satellite imagery, which maps the dominance of deposition at (Figure 10) *c–e*. Further, our simulation's depositional spread was approximately 18 hectares. Integrating this 18-hectare spread area with variable depositional thickness yielded a volume ranging from 995,580 ± 200,000 m^3 at the left flank to 1,285,260 ± 126,000 m^3 at the right flank of the debris flow deposit.

Discussion

The intense-localised antecedent precipitation of this event (Figure 5) follows a trend of similar hydrometeorological events, which are frequently linked to changing climate and its effect on the Indian summer monsoon and Western disturbance[13,15,39]. The Dharali event is a representation of a globally accelerating trend of catastrophic mass movements, such as the January 2024 Liangshui landslide in Yunnan, China[40], 2025 Los Angeles County mudslides[41], May 2025 collapse of ice and rock from the Birch glacier in Blatten, Switzerland, that highlight the growing threat from high-altitude glacial environments[42].

Despite a clear warning after the 2013 Uttarakhand floods and landslides that also affected the Kheer Gad channel[31], the institutional response was limited to the construction of retaining walls along the channel, while failing to address the unregulated land-use planning. We estimated that between 2011 and 2025, the number of built-up structures in Dharali village doubled, increasing from 89 to 160 (Figure 11). This growth, largely driven by tourism and apple orchards, led to rapid infrastructure expansion directly into vulnerable zones.

Notably, debris flow simulation's depositional spread, i.e., 18 hectares (Figure 10), compares closely with the total affected area of ~20 hectares reported in initial government documents[43]. This close match underscores the simulation's rationality for the rapid assessment of flow spread. It should be noted that a 100% match is not practical considering uncertainties in debris sources, inherent material heterogeneity, and the timing of episodic failure. Furthermore, a relatively higher volume was attained at the right flank of the deposit (Figure 10), which is supported by the field evidence suggesting more deposition (~3 m) compared to the left (Figure 3). The simulated flow height at the mouth of Kheer Gad, where the flow impacts Dharali village, was 6 m, which matches the observed field conditions (Figure 3). Furthermore, approximately 3 hectares of productive apple orchards, at least 25–30 animals, and a market comprising 65 hotels, over 30 resorts, and homestays were buried under 6–8 m of debris[44]. This deposition depth in the central part of the spread is consistent with the deposition predicted by our simulation (Figure 10 *c*). Finally, 60 kPa pressure, velocities of 5–10 m/s, and flow height of 5–10 m (Figure 6–8) were catastrophic enough to destroy the infrastructure because these values are characteristic of highly destructive, hyper-concentrated debris flows[17].

Findings also show that two key factors drove this event: (i) a landscape susceptibility to such events, as quantified by its morphometry (MRn of 0.8) (Table 2), and (ii) a trigger of antecedent rainfall (Figure 5). These morphometric conditions, combined with high antecedent rain, a moderate catchment size, and a fourth-order stream network, create a well-integrated hydrological system. This system rapidly concentrates flow energy, especially in downstream convergence sections, which can increase the probability of debris flow initiation[45]. A final, crucial factor is the abundant supply of both sediment and water from the catchment's glaciated area, which accounts for nearly 18% (~3 km^2) of the total basin. Glacial zones pose a dual threat, as they provide significant meltwater and a continuous supply of loose, unconsolidated sediments that can be readily mobilised[46]. Thus, this event demonstrates that numerous high-relief, glaciated catchments across the Himalaya may be at a tipping point, requiring mapping of sediment sources in glacial and fluvial environments, along with simulations of potential floods and landslides.

Conclusions

Our findings confirm that the study area is an inherently unstable, high-energy environment (MRn = 0.8),

primed with abundant glacial and landslide debris. We identified the trigger not as a singular event, but as an antecedent rainfall ($\sim$195 mm/30 days) that saturated the source material. The simulation's findings of 60 kPa pressure, velocities of 5–10 m/s, flow height of 5–10 m, spread area of $\sim$18 hectare, and volume of $995{,}580 \pm 200{,}000\ m^3$–$1{,}285{,}260 \pm 126{,}000\ m^3$, validated against field observations, reconstructed the event's destructive power. Ultimately, the event was not a purely natural phenomenon but a direct consequence of failed land-use planning. A doubling of infrastructure since 2011 placed the community in the direct path of a high-magnitude, quantifiable hydro-meteorological event. Future work should prioritise detailed geotechnical analysis to constrain property values for predictive modeling. A dedicated study is needed to quantify the impact of glacial retreat on the sediment budget and slope preconditioning, enabling a transition from a static assessment to a dynamic model of future hazard evolution. The present study provides a transferable methodology for assessing similar high-risk, glaciated basins and serves as a call to urgently integrate quantitative hazard science into future policy to prevent such avoidable tragedies.

Conflict of interest: The authors declare that there is no conflict of interest.

1. Nandargi, S. and Dhar, O. N., Extreme rainfall events over the Himalayas between 1871 and 2007. *Hydrol. Sci. J.*, 2011, **56**(6), 930–945.
2. Bolch, T. *et al.*, The state and fate of Himalayan glaciers. *Sci.*, 2012, **336**(6079), 310–314.
3. Kulkarni, A. V. and Karyakarte, Y., Observed changes in Himalayan glaciers. *Curr. Sci.*, 2014, **106**(2), 237–244.
4. Bharti, V., Aingh, C., Ettema, J. and Turkington, T. A. R., Spatiotemporal characteristics of extreme rainfall events over the Northwest Himalaya using satellite data. *Int. J. Climatol.*, 2016, **36**(12), 3949–3962.
5. Sundriyal, Y., Kaushik, S., Kumar, V., Dimri, A. P., Chauhan, N., Kumar, S. and Rana, N., Uttarakhand: a hotspot for extreme events?, *J. Geol. Soc. India*, 2025, **101**(7), 1120–1126.
6. Dobhal, D. P., Gupta, A. K., Mehta, M. and Khandelwal, D. D., Kedarnath disaster: facts and plausible causes. *Curr. Sci.*, 2013, **105**(2), 171–174.
7. Wasson, R. J., Sundriyal, Y. P., Chaudhary, S., Jaiswal, M. K., Morthekai, P., Sati, S. P. and Juyal, N., A 1000-year history of large floods in the upper Ganga catchment, central Himalaya, India. *Quat. Sci. Rev.*, 2013, **77**, 156–166.
8. Ziegler, A. D. *et al.*, Pilgrims, progress, and the political economy of disaster preparedness-the example of the 2013 Uttarakhand flood and Kedarnath disaster. *Hydrol. Process.*, 2014, **28**(24), 5985–5990.
9. Uttarakhand Information Commission, Press Releases; https://uttarainformation.gov.in/press.php (accessed on 1 September 2025).
10. Hewitt, K., The Karakoram anomaly? Glacier expansion and the'elevation effect,' Karakoram Himalaya. *Mt. Res. Dev.*, 2005, **25**(4), 332–340.
11. Shugar, D. H. *et al.*, A massive rock and ice avalanche caused the 2021 disaster at Chamoli, Indian Himalaya. *Sci.*, 2021, **373**(6552), 300–306.
12. Bookhagen, B. and Burbank, D. W., Toward a complete Himalayan hydrological budget: spatiotemporal distribution of snowmelt and rainfall and their impact on river discharge. *J. Geophys. Res.: Earth Surf.*, 2010, **115**(F3), 1–25.
13. Rajeevan, M., Gadgil, S. and Bhate, J., Active and break spells of the Indian summer monsoon. *J. Earth Syst. Sci.*, 2010, **119**(3), 229–247.
14. Sundriyal, Y. *et al.*, Impact of potential flood on riverbanks in extreme hydro-climatic events, NW Himalaya. *Bull. Eng. Geol. Environ.*, 2023, **82**(6), 1–18.
15. Kumar, V. *et al.*, Ascertaining potential causes of hillslope failure associated to human settlement: a case study from Alaknanda valley, Uttarakhand, NW Himalaya, India. *J. Geol. Soc. India*, 2023, **99**(8), 1141–1148.
16. Sundriyal, Y., Kumar, V., Chauhan, N., Kaushik, S., Ranjan, R. and Punia, M. K., Brief communication: the northwest Himalaya towns slipping towards potential disaster. *Nat. Hazards Earth Syst. Sci.*, 2023, **23**(4), 1425–1431.
17. Chauhan, N., Kumar, V., Sundriyal, Y., Kaushik, S., Subramanian, S. S., Melo, R. and Rana, N., Debris flow in indian himalaya: a threat to emerging infrastructure. *Bull. Eng. Geol. Environ.*, 2024, **83**(11), 428.
18. Horton, R. E., Erosional development of streams and their drainage basins; hydrophysical approach to quantitative morphology. *Bull. Geol. Soc. Am.*, 1945, **56**(3), 275–370.
19. Schumm, S. A., Evolution of drainage systems and slopes in badlands at Perth Amboy, New Jersey. *Geol. Soc. Am. Bull.*, 1956, **67**(5), 597–646.
20. Melton, M. A., The geomorphic and paleoclimatic significance of alluvial deposits in southern Arizona. *J. Geol.*, 1965, **73**(1), 1–38.
21. Church, M. and Mark, D. M., On size and scale in geomorphology. *Prog. Phys. Geogr.*, 1980, **4**(3), 342–390.
22. Miller, J. R., Ritter, D. F. and Kochel, R. C., Morphometric assessment of lithologic controls on drainage basin evolution in the Crawford Upland, south-central Indiana. *Am. J. Sci.*, 1990, **290**(5), 569–599.
23. Rickenmann, D., Empirical relationships for debris flows. *Nat. hazards*, 1999, **19**(1), 47–77.
24. Hungr, O., A model for the runout analysis of rapid flow slides, debris flows, and avalanches. *Can. Geotech. J.*, 1995, **32**(4), 610–623.
25. Crosta, G. B., Imposimato, S. and Roddeman, D., Numerical modelling of entrainment/deposition in rock and debris-avalanches. *Eng. Geol.*, 2009, **109**(1–2), 135–145.
26. Christen, M., Kowalski, J. and Bartelt, P., RAMMS: Numerical simulation of dense snow avalanches in three-dimensional terrain. *Cold Reg. Sci. Technol.*, 2010, **63**(1–2), 1–14.
27. Frank, F., McArdell, B. W., Huggel, C. and Vieli, A., The importance of entrainment and bulking on debris flow runout modeling: examples from the Swiss Alps. *Nat. Hazards Earth Syst. Sci.*, 2015, **15**(11), 2569–2583.
28. Grelle, G., Rossi, A., Revellino, P., Guerriero, L., Guadagno, F. M. and Sappa, G., Assessment of debris-flow erosion and deposit areas by morphometric analysis and a GIS-based simplified procedure: a case study of Paupisi in the southern Apennines. *Sustainability*, 2019, **11**(8), 1–20.
29. Valdiya, K. S., *Dynamic Himalaya*, Universities Press, Hyderabad, 1998, pp. 1–178.
30. Hodges, K. V., Tectonics of the Himalaya and southern Tibet from two perspectives. *Geol. Soc. Am. Bull.*, 2000, **112**(3), 324–350.
31. Bhambri, R., Mehta, M., Tiwari, S. K., Yadav, J. S. and Sain, K., High mountain hazards in Uttarakhand. In *Geo-information for disaster monitoring and management*, Springer International Publishing, Cham, Switzerland, 2024, pp. 181–210.
32. McNally, A. *et al.*, A land data assimilation system for sub-Saharan Africa food and water security applications. *Sci. data*, 2017, **4**(1), 1–19.
33. Kumar, V., Jamir, I., Gupta, V., and Bhasin, R. K., Inferring potential landslide damming using slope stability, geomorphic constraints, and run-out analysis: a case study from the NW Himalaya. *Earth Surf. Dynam.*, 2021, **9**(2), 351–377.

34. RAMMS: Debris Flow. Rapid Mass Movement Simulation. https://ramms.ch/ramms-debrisflow/ (accessed on 1 September 2025).
35. National Database for Emergency Management, UK Flood 5.0 (VAP-2) Report. NRSC, ISRO, 2025; https://ndem.nrsc.gov.in/documents/Disaster_Document/2025/UK/ukflood50dsc07082025/ukflood50dsc07082025_vap2.pdf (retrieved on 20 August 2025).
36. Wilford, D. J., Sakals, M. E., Innes, J. L., Sidle, R. C. and Bergerud, W. A., Recognition of debris flow, debris flood and flood hazard through watershed morphometrics. *Landslides*, 2004, **1**(1), 61–66.
37. Marchi, L. and Dalla Fontana, G., GIS morphometric indicators for the analysis of sediment dynamics in mountain basins. *Environ. Geol.*, 2005, **48**(2), 218–228.
38. Berti, M. and Simoni, A., Experimental evidences and numerical modelling of debris flow initiated by channel runoff. *Landslides*, 2005, **2**(3), 171–182.
39. Prakash, S. and Srinivasan, J., A comprehensive evaluation of near-real-time and research products of IMERG precipitation over India for the southwest monsoon period. *Remote Sens.*, 2021, **13**(18), 1–19.
40. Wang, W., Ma, S., Yan, W. and Yuan, R., The spatial distribution characteristics and possible influencing factors of landslide disasters in the Zhaotong area, Yunnan province of China. *Appl. Sci.*, 2024, **14**(12), 1–14.
41. Thomas, M. A., Michaelis, A. C., Oakley, N. S., Kean, J. W., Gensini, V. A. and Ashley, W. S., Rainfall intensification amplifies exposure of American Southwest to conditions that trigger postfire debris flows. *Nat. Hazards*, 2024, **1**(1), 1–10.
42. Allen, S. K., Rastner, P., Arora, M., Huggel, C. and Stoffel, M., Lake outburst and debris flow disaster at Kedarnath, June 2013: hydrometeorological triggering and topographic predisposition. *Landslides*, 2016, **13**(6), 1479–1491.
43. Indian satellite data based analysis of the Dharali flash flood. ISRO, 2025; https://www.isro.gov.in/indian_satellite_data_based_analysis_of_the_dharali_flash_flood.html (retrieved on 10 October 2025).
44. Singh, A. P., Dharali calamity destroyed livestock, 3 hectares of agriculture land. Garhwal Post, 2025; https://garhwalpost.in/dharali-calamity-destroyed-livestock-3-hectares-of-agriculture-land (retrieved on 20 August 2025).
45. Cavalli, M., Trevisani, S., Comiti, F. and Marchi, L., Geomorphometric assessment of spatial sediment connectivity in small Alpine catchments. *Geomorphology*, 2013, **188**, 31–41.
46. Sonkar, G., Rana, N., Kumar, H., Sharma, S., Kumar, V. and Sundriyal, Y., Assessing flash flood hazard and buildings exposure in the Himalayan upland region: a case study of Gangotri Town, India. *Z. fur Geomorphol.*, 2025; doi: 10.1127/zfg/2025/0800.

ACKNOWLEDGEMENT. The authors are thankful for the financial support from the Ministry of Earth Sciences, Government of India, New Delhi [Ref. No.: MOES/P.D.(Seismo)MOES-UKRI (14965)/2024].

Received 19 November 2025; accepted 7 January 2026.

doi: 10.18520/cs/v130/i3/229-238